Proceedings of McMat2005:
2005 Joint ASME/ASCE/SES Conference on Mechanics and Materials
June 1 - 3, 2005, Baton Rouge, Louisiana, USA

624

Geometrically Constrained Flow Behavior with Uniform Disks

Hayley H. Shen/Clarkson University **James T. Jenkins/Cornell University**

Shunying Ji/Clarkson University

ABSTRACT
A simple shear flow of granular materials is studied to determine the stress and strain rate relation under high concentration. It is found that grain structure may form under slow shear rates so that a narrow shear band accommodates all shearing motion. Accompanying such structures is a periodic progression of stresses. The formation and stability of the shear band depends on both the shear rate and the sample size. At high shear rate and large sample size, stable structures give way to random organizations and random stress fluctuations. In a dense granular flow, a minimum number of particle layers are required to re-organize, in order to create space for the shear band. For sample sizes comparable to the required number of layers for a shear band to exist, only one shear band is possible, hence the integrity of this shear band persists into lower concentration. As the sample size increases, several shear bands may co-exist in the aggregate. These shear bands may merge into a chaotic, low concentration band, where a collisional granular shear flow appears. From these observations one naturally questions the existence of a constitutive law for such highly concentrated flows at low shear rates. It seems that only for large-scale problems, where this geometric constraint is no longer a factor, can one obtain true constitutive relations for granular flows. The observations made are based on computer simulations of uniform disks. For poly-dispersed systems, we speculate that the same phenomena exist for narrow size distributions and will disappear when the size distribution is broad.

INTRODUCTION
Numerical simulations of simple shear flows with periodic boundary condition have been used to establish the constitutive relation of a granular assembly. The effect of sample size on the results has been mentioned for both 2D (Babic et al., 1990; Shen, 2001) and 3D systems (Campbell, 2002). In a 2D simulation with a small sample size and high concentration, the discs quickly arrange themselves into a hexagonal packing in which shear occurs over a single rolling layer of discs. The average stresses are independent of the shear rate, but experience large periodic oscillations, with a frequency directly related to the shear rate. With decreasing concentration or increasing sample size, both the hexagonal regular packing and the periodic stress oscillations gradually give way to random packing and randomly fluctuating stresses. The average stresses become increasingly dependent on the shear rate. Campbell (2002) characterized the transition from rate-independent to rate-dependent regimes for dense 3D systems of various material properties.

In nearly static situations, Howell et al. (1999) studied both 2D and 3D systems in physical experiments and found that for large systems stress fluctuations can exist for dense slow granular materials, even though the spatial disorder of grains is small.

From these studies, it is clear that in dense granular flows, orderly motion with shearing taking place in localized regions is a preferred mode. Under such orderly shearing, the stresses progress with regularity. The first indication of the deterioration of such orderly motion is random fluctuations of the stresses. With increasing sample size or shear rate, increasing stress randomness precedes the spatial disorder. To understand the slow dense flow of granular materials it is interesting to determine what controls their organization ability.

In this work, we study the spatial organization of a granular assembly under shear. The effect of sample size, shear rate and friction coefficient are investigated. With a high concentration, we believe that the geometric constraint plays an important role. We will examine the formation of regular packing, the shear bands, the associated stress fluctuations, and the rate dependency of the average stresses on the shear rate. A uniform disc assembly sheared under periodic boundary conditions will be our model.

Our conceptual idea is explained as follows. At high solid concentration granular materials can shear only if enough space is created in the aggregate. This space can be created by compressing particles or by re-organizing them. The former creates high stresses, the latter requires time. When the shear rate is low, the grains have sufficient time to re-organize to accommodate shear. For aggregates of uniform disks, the size of the groups perpendicular to the shearing direction may be calculated from pure geometric arguments. At fixed shear rate, as the solid concentration gradually decreases more random motions among the particles become possible. The stability of the tightly packed region decreases. Shearing zones begin to jump around the aggregate in a chaotic fashion. Eventually, at low enough concentration, grain order gives way to a fully random spatial distribution.

NOMENCLATURE

a, b horizontal and vertical sample size
B Dimensionless shear rate
C Concentration Na Horizontal particle number
d Particle diameter
dt Time step
e Restitution coefficient
Kn Normal stiffness
Ks Shear stiffness
m Particle mass
Shear rate
Nb Vertical layer number
V, H Vertical and horizontal distances between layers
μ Friction coefficient

1. Analysis of periodic sliding

Consider a shear flow moving in the horizontal direction with a gradient in the vertical direction as shown in Fig. 1. In dense granular flows, shear occurs in very narrow localize regions. The most extreme case is a shear band that consists of a single sliding plane with a width of a single particle diameter as in Fig. 1(a). This situation occurs for nearly frictionless materials. For sufficiently frictional materials, rolling instead of sliding occurs in the shear band. The smallest width of this type of shear band is two-particles, as in Fig. 1(b).

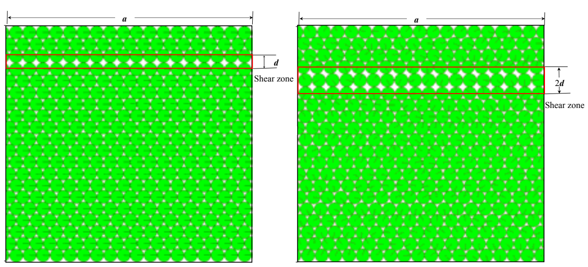

(a) 1 layer (sliding) (b) 2 layers (rolling)

Fig. 1 Minimum shear bands.

We start with a given concentration C_0 and a sample size of a (horizontal) and b (vertical) layers. Imagine a regular packing as in Fig. 2(a). When the concentration is less than the maximum possible value, there is a small gap between neighboring particles. When shearing motion begins, if the density is high, the particles will run into each other. Under very slow flow, particles are able to group together to create a low concentration zone where shear may occur without large compression of particles. We are interested in finding the number of particles that need to group together to form this shear band.

Fig. 2(b) shows the geometric arrangement between a particle in the shear band, and the immediate neighbors above it. The re-arrangement required to create a shear band will force the particles to pack more tightly in the vertical direction while leave the horizontal distance between particles in the shear band the same as before the shear. Simple geometric manipulation yields: $C_{\max} = \sqrt{3}\pi/6$, $H_{\min} = 2r$, $V_{\min} = \sqrt{3}r$, $H_0 = 2r\sqrt{C_{\max}/C_0}$, and $V_0 = \sqrt{3}H_0/2$. The particle numbers in the sample N_a an N_b are related to the sample size as $a = N_a \times H_0$ and $b = N_b \times V_0$, where r is the particle radius. V_s and $H_0 = H_s$.

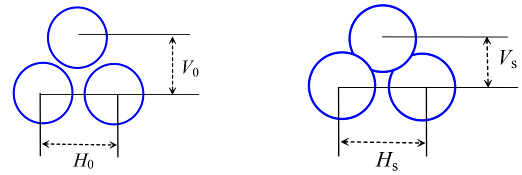

(a) at concentration C_0; (b) at concentration C_s.

Fig. 2 Definition of geometrical variables in periodic-sliding process.

(1) Minimum layer number versus concentration with non-overlapping particles

When the shear rate approaches zero, the particle system has enough time to re-organize. We consider the minimum shear band cases: Fig. 1(a, b). If particles do not overlap in the assembly, for a sliding shear band (as Fig. 1(a)), we have

$$N_b = \frac{d - V_s}{V_0 - V_s} = \frac{2 - 1\sqrt{4 - \frac{C_{\max}}{C_0}}}{\sqrt{\frac{3C_{\max}}{C_0}} - \sqrt{4 - \frac{C_{\max}}{C_0}}} \tag{1}$$

For a rolling shear band (as Fig. 1(b)), we have

$$V_s = \sqrt{d^2 - \left(\frac{H_s}{2}\right)^2} = r\sqrt{4 - \frac{C_{\max}}{C_0}} \tag{2}$$

$$(N_b - 2) * V_s + 2d = b \tag{3}$$

Substituting Eq. (2) into Eq. (3), we have

$$N_b = \frac{2(d - V_s)}{V_0 - V_s} = \frac{4 - 2\sqrt{4 - \frac{C_{\max}}{C_0}}}{\sqrt{\frac{3C_{\max}}{C_0}} - \sqrt{4 - \frac{C_{\max}}{C_0}}} \tag{4}$$

The results are plotted in Fig. 3 versus concentration.

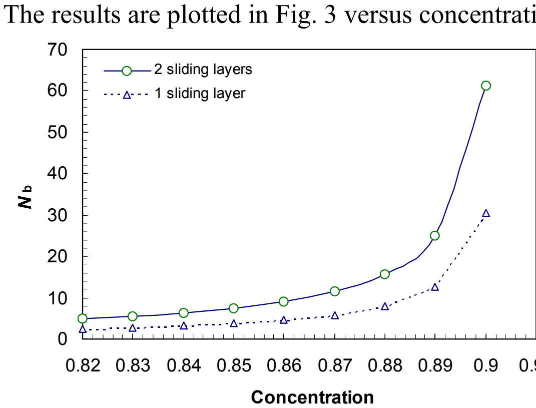

Fig. 3 Minimum layer number vs. concentration.

(2) Maximum overlap versus sample size

Considering the rolling shear band in Fig. (1b), based on Eq. (3), we have

$$V_s = \frac{b-2d}{N_b - 2} \tag{5}$$

Substituting $b = N_b \times V_0 = \sqrt{3} r N_b \sqrt{\frac{C_{max}}{C_0}}$ into Eq. (5) yields

$$V_s = \frac{\left(\sqrt{3} N_b \sqrt{\frac{C_{max}}{C_0}} - 4\right) r}{N_b - 2} \tag{6}$$

for 1 sliding layer, we have

$$V_s = \frac{\left(\sqrt{3} N_b \sqrt{\frac{C_{max}}{C_0}} - 2\right) r}{N_b - 1} \tag{7}$$

The maximum overlap in the regular sliding can be estimated as

$$x = d - \sqrt{\frac{h_s^2}{4} + V_s^2} \tag{8}$$

The maximum overlaps in sliding under different particle layers are plotted in Fig. 4 for $C_0 = 0.90$ and 0.89. The overlap decreases as the sample size increase. Peak stress during a shear cycle will also decrease and the overlap reduces. When the sample size is large enough, there is no overlap anymore. When this happens, regular sliding is no longer needed to facilitate the shear. The shearing motion will become more random and stresses will display fluctuations and rate dependency.

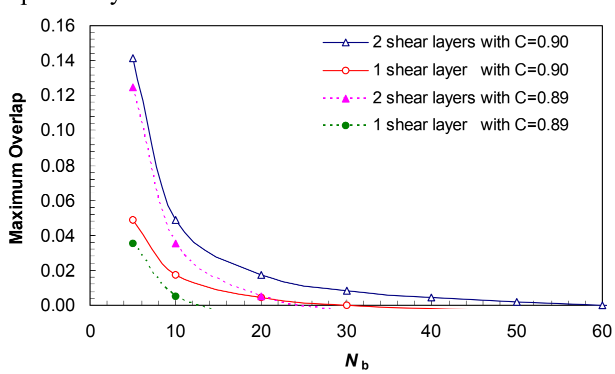

Fig. 4 Maximum overlap in different sample size under regular shear band.

(3) Localized concentration versus sample size

Inside the shear band the local concentration is lower than the mean concentration. The remaining assembly has a concentration C_s higher than the mean C_0. For sliding shear band shown in Fig. 1(a), we have

$$C_s a(b-d) = N_a (N_b - 2)\pi r^2 \tag{9}$$

i.e. $$C_s = \frac{N_a (N_b - 2)\pi r^2}{a(b-d)} = \frac{(N_b - 1)\pi r^2}{H_0 (N_b V_0 - 2r)} \tag{10}$$

Similarly, for the rolling shear band shown in Fig. 1(b)

$$C_s = \frac{(N_b - 2)\pi r^2}{H_0 (N_b V_0 - 4r)} \tag{11}$$

Based on Eqs. (10) and (11), the localized concentration can be determined for the sliding and rolling shear bands for different sample sizes N_b, respectively. The results are plotted in Fig. 5.

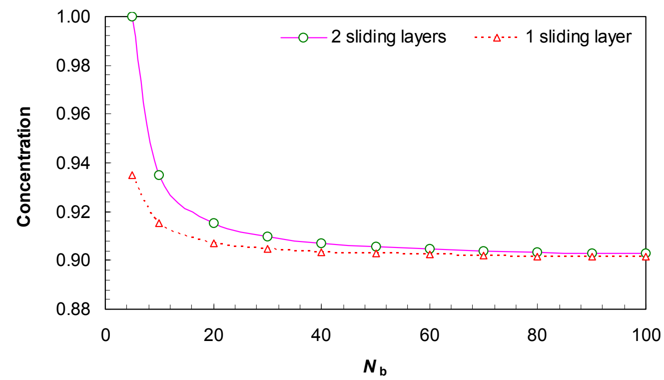

Fig. 5 Local concentration vs. layer number.

The results in Figs. 3 to 5 are obtained under the assumption that the entire sample is in a static state. When the shear rate is extremely slow the particle system have enough time to re-organize into the "most favorable" conditions shown in Fig. 1. These conditions will not be possible if the sample size is smaller than the required value shown in Fig. 3.

2. Dynamic properties of particle system under shear

We will next study the dynamic behavior of a sheared assembly. The parameters used are given in Table 1 unless otherwise specified. We apply the usual periodic boundary condition. The dimensionless shear rate is defined as $B = \dot{\gamma} / \sqrt{K_n / m}$.

Table 1. Parameters in the 2D granular flow simulation with periodic boundary

Variable	Definition	values
N_a	Horizontal particle number	20
N_b	Vertical layer number	20
K_n	Normal stiffness	1.0×10^6
m	Particle mass	1.0
$\dot{\gamma}$	Shear rate	0.1
B	Dimensionless shear rate	1.0×10^{-4}
μ	Friction coefficient	0.5
e	Restitution coefficient	0.9
K_s	Shear stiffness	8.0×10^5
d	Particle diameter	1.0
dt	Time step	$T_{bc}/50$
C	Concentration	0.90

With the given sample size and friction, shear occurs in a rolling band as in Fig. 1(b). The simulated dimensionless stress

$\tau_{ij}^{*} = \tau_{ij} / \left(\rho D^2 \dot{\gamma}^2\right)$ is plotted in Fig. 6. All three components of the stresses change periodically with time. The period is exactly the time required to move the regular packing above and below the rolling layer a distance H_0. The magnitude of maximum stress τ_{22}^{*} is much larger than τ_{11}^{*} because the compression between particles are dominant in the vertical direction.

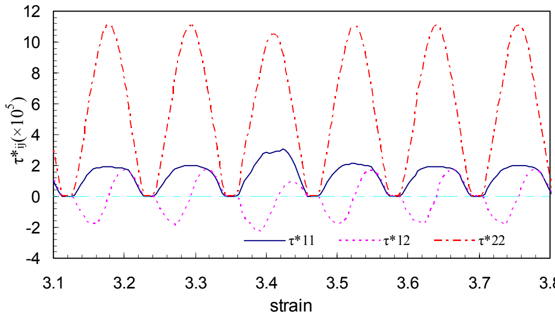

Fig. 6. Simulated results with C=0.9 (sample size: $N_a \times N_b$=20×20).

We introduce two more tests to compare with the base case shown above. In case (a) we reduce the concentration from 0.90 to 0.89, in case (b) we reduce the sample size $N_a \times N_b$ from 20×20 to 10×12. All other parameters are the same as those listed in Table 1. We find that in case (a) the shear zone remains as a rolling layer. The simulated stresses are plotted in Fig.7 (a). The stress magnitude reduces to 1/4 of that when concentration was 0.90. At the same time, the normal stresses begin to lose their regular periodicity. The positive portion of the shear stress weakens. If we further reduce the concentration, the positive portion of shear stress vanishes. In case (b), the stress periodicity remains the same as in the original case, while the magnitude of stresses nearly doubles. Moreover, we also find that the shear band changes from rolling to sliding. From this observation we expect that the width of a shear band will increase with the sample size.

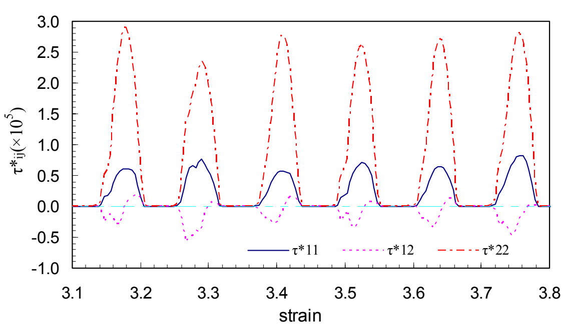

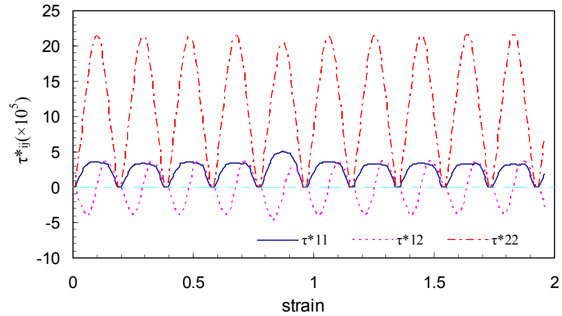

Fig. 7. Simulated dimensionless stresses with (a) C=0.89, $N_a \times N_b$=20×20 and (b) C=0.90, $N_a \times N_b$=10×12.

3. Critical conditions for periodic stresses

The stability of shear band appears to be related to the stress state. As the stresses begin to deviate from periodic, the shear band begins to widen. In this section we will discuss the transition from periodic to random stress fluctuations for different sample sizes, shear rates, concentrations, and friction coefficients. In the following, the computational parameters are the same as listed in Table 1, unless specified otherwise.

3.1 Test on sample size N_b

To test the effect of sample size, we let N_b vary from 4 to 100 and fix N_a at 20. The averaged τ_{22}^{*} and the amount of overlap are plotted in Fig. 8. The amount of overlap from the simulation under this slow shear rate is close to the analytical solution given in Eq. (8). The simulated stress τ_{22}^{*} has the same decreasing trend as the sample size increases. When we examined the flow using animation, we found that a stable shear band existed when 7<N_b<50. When N_b < 7, the granular assembly does not have enough space to generate periodic sliding, and the shear zone spreads over the whole domain. When N_b > 50, the shear zone occurs in several layers, and the stresses fluctuate wildly as shown in Fig. 9. Large stress fluctuations in moderately large system have also been found in physical experiments (Howell et al., 1999; Mueth et al., 1998).

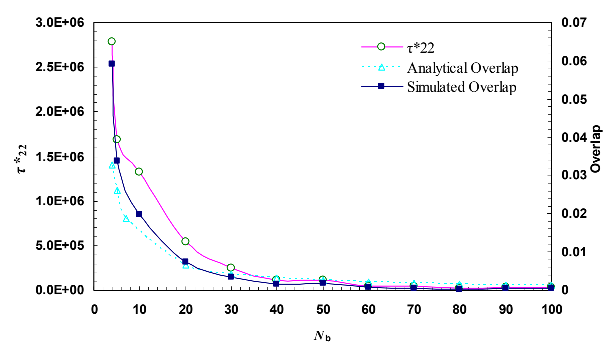

Fig. 8 Overlap and stress τ_{22}^{*} versus sample size.

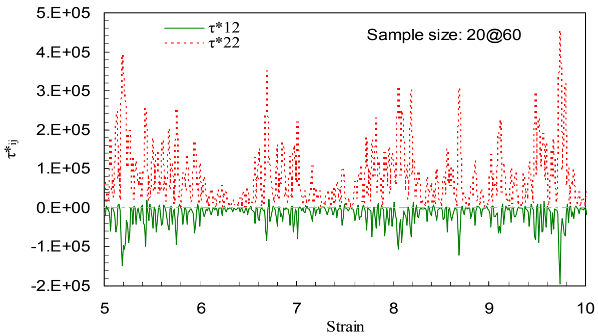

Fig. 9 Fluctuation of τ^*_{12} and τ^*_{22}.

3.2 Test on shear rate

Results for different shear rates are given in Fig. 10 where $\dot{\gamma}$ = 0.1, 0.5, 1.0 and 5.0. The mean dimensionless stresses show that when $\dot{\gamma}$ < 0.5 ($B < 5\times10^{-3}$), the particle system undergoes regular shearing. With an increasing shear rate, the periodicity of the stress deteriorates. When $\dot{\gamma}$ > 5.0, all trace of periodicity is lost in the stress.

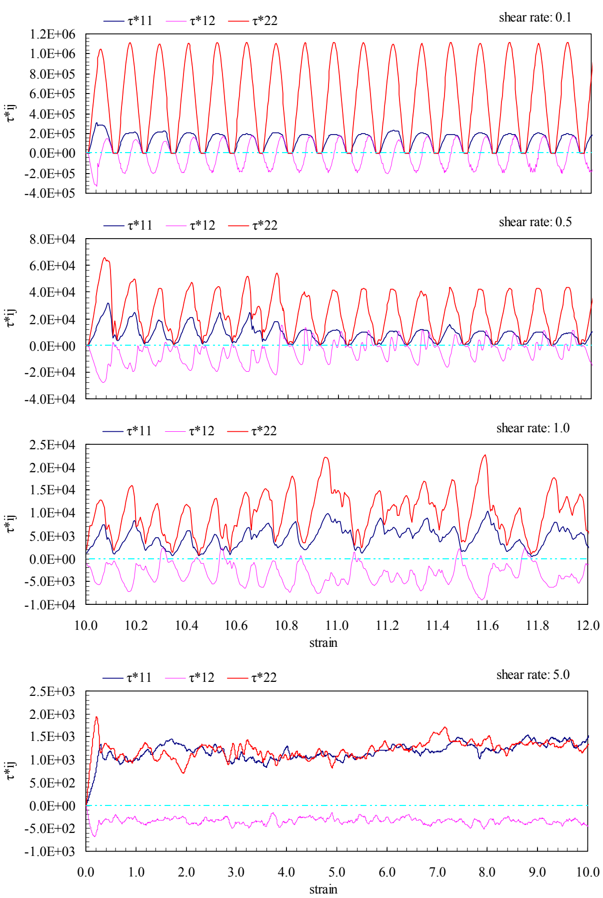

Fig. 10 simulated stress for different shear rates.

3.3 Test on concentration

The averaged dimensionless stresses associated with reducing concentration from 0.90 to 0.80 are plotted in Fig. 11. As the concentration decreases, the stresses exhibit a very surprising minimum between C =0.88 and 0.87. In order to explain this odd phenomenon, an animation of the particle movement and the stress fluctuations was examined. From the motion of particles, we found regular sliding under dense condition ($C \geq 0.87$), and random motion random under the loose condition ($C \leq 0.86$).

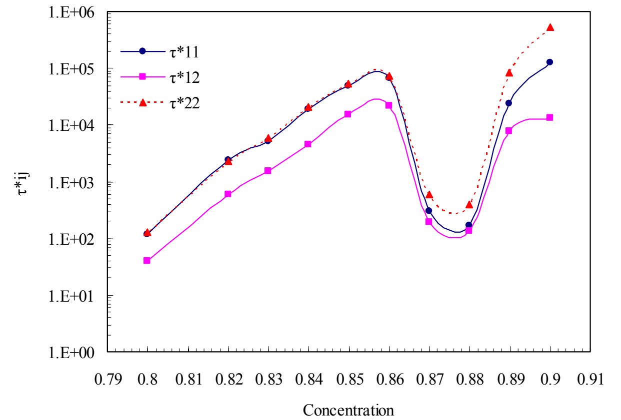

Fig. 11 Averaged τ^*_{ij} versus concentration.

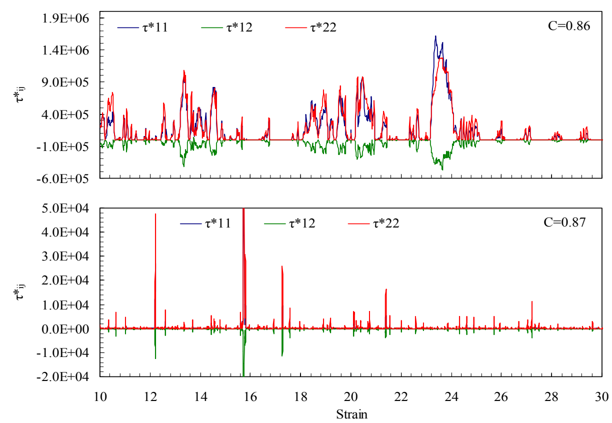

Fig.12 Fluctuation of τ^*_{ij} for C=0.86 and 0.87.

We study two concentrations, C = 0.86 and 0.87, one inside the minimum stress region and one outside of it. The graph of the stress in Fig. 12 shows that in both cases τ^*_{ij} experiences strong fluctuations, but the stress pulses of C = 0.87 are much narrower than C = 0.86. Two typical snapshots of the particle configuration in these two cases are given in Fig. 13. It is clear that the shear zone is very narrow for C = 0.87. Hence particle rearrangement is easy. This can also explain the narrow stress pulses and rapid force chain collapse. For C = 0.86, the shear banding is complex and the bands more numerous. Re-organization of particles is difficult. Particles remain in long contact and thus stress pulses are longer, resulting in larger average stress too.

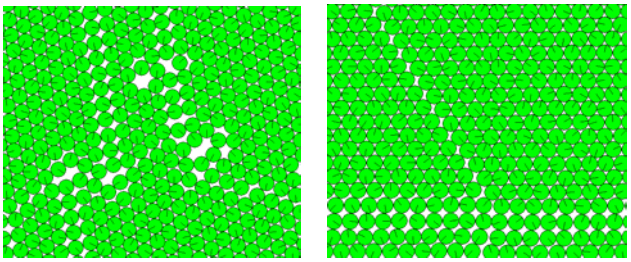

***C*=0.86** **_C_=0.87**

Fig. 13 Particle configurations in random shear flow (*C*=0.86) and regular shear flow (*C*=0.87).

In the simulation above, the sample size is 20×20. If the sample size increases to 20×100, the results show that there is no clear transition between random and regular shearing motion (Fig. 14). Thus, the influence of geometrical constraints becomes weaker as the sample size grows. We also expect such constraints to be less prominent in 3D due to the greater number of degrees of freedom.

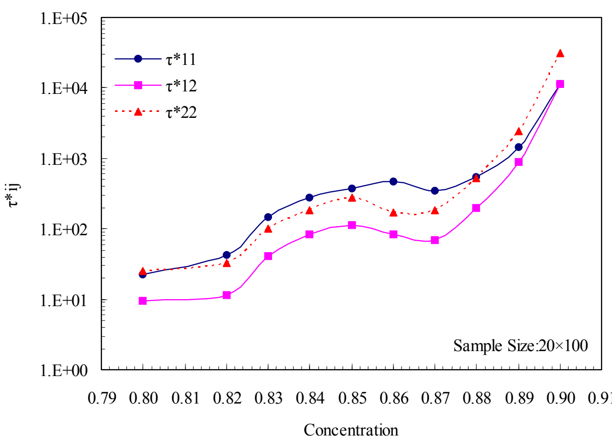

Fig. 14 Averaged τ_{ij}^* in steady state versus concentration.

3.4 Test on friction coefficient

The effect of friction coefficient on the shear band behavior is shown in this section. When μ < 0.80, the particle system appears to perform regular layered-shear motion as in Fig. 1(b). The resulting stresses are periodic. When $\mu \geq 0.80$, the particles can be sheared in layers, but the stress frequency and amplitude are no longer steady. When μ ≥ 0.90, the granular system becomes completely random. The average stresses versus friction coefficient are shown in Fig. 15. In the range $0.2 \leq \mu \leq 0.8$, the dimensionless stresses are independent of the friction coefficient. In this case the stresses are dominated by the compressive stresses created when particles overlap each other in the rolling shear. From the animation, we also find that there is only one shear band for friction coefficients μ = 0.0 and 0.1, while there are two shear bands when $0.2 \leq \mu \leq 0.8$.

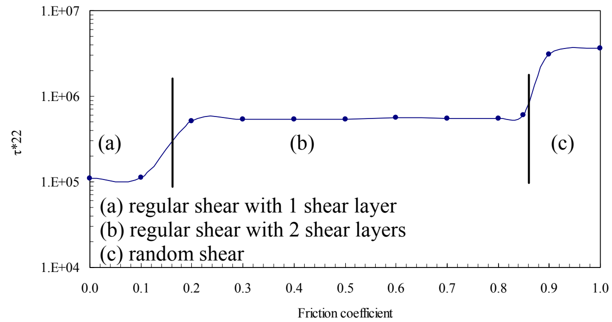

Fig. 15 Averaged stress versus friction coefficient.

4. Conclusions

In the slow dense granular materials, the geometric constraint on the shear flow behavior is studied with a series of numerical simulations. These simulations use an assembly of uniform disks. The relationships among stresses, shear rate, sample size, and concentration are analyzed. The regular motion of packed material over a narrow shear band is found to be a norm when shear rate is low and sample size is over a critical value. It is found that such regular motion can be generated more easily for dense and slow flows, because there is enough time and strong constraint for particle to re-organize. This re-organization tends to minimize the normal stress, particle compression and the potential energy in the system. If the sample size is too large or too small, the particle motion and configuration become random. The transition between regular and random shear motion is less sharp with a large sample size. When particle friction increases the shear band also widens. Although this study is based on uniform particles, we believe that most of the phenomena will persist even for mildly poly-disperse systems. The formation of particle grouping and narrow shear band appears to be the only way dense granular flows can accommodate shear motion. The stability of the groups and shear bands are closely related to the stress fluctuations and the rate-dependence of the stresses.

ACKNOWLEDGMENTS

This study is supported in part by NASA Microgravity Fluid Physics Program grant number NAG3-2717.

REFERENCES

1. Babic M and Shen H. H. Shen. The stress tensor in granular shear flows of uniform, deformable disks at high solids concentrations. Journal of Fluid Mechanics, 1990, 219: 81-118.
2. Campbell C. Granular shear flows at the elastic limit. Journal of Fluid Mechanics, 2002, 465: 261-291.
3. Howell D W, Behriger R P, Veje C T. Fluctuations in granular media. Chaos, 1999, 9(3): 559-572.
4. Mueth D M, Jaeger H M, Nagel S R. Force distribution in a granular medium. Physical Review E, 1998, 57(3): 3164-3169.
5. Shen H H. Sample size effects on constitutive relations of granular materials – a numerical simulation study with two-dimensional flow of disks. Journal of Engineering Mechanics, 2001, 978-986.